OPTIMIZING MEMBRANE CHARACTERIZATION USING THE DATA (DIAFILTRATION APPARATUS FOR HIGH-THROUGHPUT ANALYSIS) FRAMEWORK

Xinhong Liu, Jonathan A. Ouimet, Laurianne Lair, William A. Phillip and Alexander W. Dowling[*]
Department of Chemical and Biomolecular Engineering, University of Notre Dame
Notre Dame, IN 46556

Abstract

Membrane characterization provides essential information for the scale-up, design, and optimization of new separation systems. We recently proposed the Diafiltration Apparatus for high-Throughput Analysis (DATA) framework, which enables a 10-times reduction in the time necessary to characterize neutral membrane transport properties by integrating experiments, a new sensor, dynamic modeling, and parameter estimation. In this work, we extend the DATA framework to consider charged membranes. We postulate different physics-informed models to capture the concentration-dependent membrane performance. Using the tools of data science, we intelligently compare these model alternatives, and show that the solute permeability coefficient of NF270 membranes exhibits quadratic behaviors as a function of upstream conditions. Moreover, we extend the modeling framework to consider experiment start-up to leverage additional data to elucidate the physical system and improve the parameter precision. Using Fisher information matrix (FIM) analysis, we quantitatively compare the information gained for different experimental operating modes, i.e., "lag" or "overflow" startup. Additionally, a time correction for permeate product collected is introduced to improve the model predictions. Finally, we use model-based design of experiments (MBDoE) techniques to contemplate the benefits of modulating the applied pressure during experiments.

Introduction

As their applications continue to expand, membrane processes have improved the sustainability and energy efficiency of modern separations. To achieve separations of similar-sized molecules with higher selectivity, the recent material design efforts focus on two directions: the precise control of membrane nanostructures and the identification of chemical functions that highlight the desired transport properties (Hoffman and Phillip, 2020; Sadeghi et al., 2018). A detailed and realistic description of the underlying thermodynamic and transport phenomena can elucidate the molecular interactions and mechanisms that affect the macroscopic performance of membranes (Geise et al., 2014; Yaroshchuk et al., 2018). In this regard, developing membrane characterization techniques that explore the dependency of membrane transport properties on upstream conditions can greatly accelerate the development of new

---

[*] To whom all correspondence should be addressed, adowling@nd.edu

materials (Ghosh et al., 2000). Furthermore, membrane characterization elucidating the underlying mechanism provides essential and reliable information for scale-up, design, and optimization, facilitating the development of separation systems.

Design of Experiments (DoE) methods optimize (computational or physical) experiments to maximize the information gain and minimize time and resource costs in a way that facilitates statistical inference. Classical "black-box" DoE approaches such as factorial designs or response surface methods explore the input-output relationship without directly exploiting scientific knowledge. In contrast, model-based DoE (MBDoE) leverage high-fidelity models constructed from underlying scientific principles, to optimize experimental campaigns that discriminate between scientific hypotheses (posed as mathematical models) or improve parameter estimation precision (Franceschini and Macchietto, 2008). The emergence of new MBDoE software (Wang and Dowling, 2022) has great potential to optimize the design of instruments and experimental conditions to better characterize the performance of separation devices as a function of operating conditions (e.g., feed concentrations) in complex feed streams. However, to date, their application to problems in membrane science remains limited.

We recently proposed the automated Diafiltration Apparatus for high-Throughput Analysis (DATA), which enables a 10-times reduction in the time, realized with fewer experiments necessary to characterize the transport properties of neutral membranes (Ouimet et al., 2022; Muetzel et al., 2022). In a subsequent conference paper, we mathematically quantified these improvements in the form of information gain using MBDoE and further refine the static (i.e., time-invariant) experimental conditions for DATA to characterize the transport properties of neutral membranes (Liu et al., 2022). In this presentation, we quantify the prediction improvements and information gain from modeling process startup.

Methods

In the dynamic diafiltration experiments deployed in the DATA framework (Ouimet et al., 2022) and shown in Figure 1, a concentrated diafiltrate is continuously injected into a stirred cell under applied pressure, ΔP, and the resulting permeate is collected in several scintillation vials. The mass of the sample vial, m_v, and the concentration of retentate in the stirred cell, c_f, are measured at a rate of 0.2 Hz while the final concentration in the sample vial, c_v, is measured for every 1 g permeate.

Using these measurements, three model parameters are estimated via a weighted least-square nonlinear regression problem in Eq. (1), $\theta = \{L_p, B, \sigma\}$: (i) hydraulic permeability, L_p; (ii) the solute permeability coefficient, B; and (iii) the reflection coefficient, σ . Both L_p and B correspond to the membrane transport properties while σ

depends on the thermodynamics of the membrane-solution interface. Here each type of data is normalized by the weight $w_{m_{v,i}}$, $w_{c_{v,j}}$, and $w_{c_{f,k}}$. These parameters are related to the volumetric flux of water, J_w, and the molar flux of the solute, J_s, across the membrane in Eqs. (2) & (3), where ΔP and $\Delta \pi$ are the applied pressure and osmotic pressure, b_i is the factor associated with ith order of c_f, respectively.
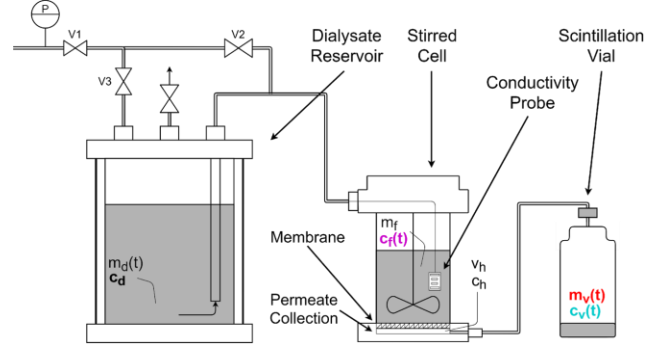

Figure 1. Dynamic diafiltration apparatus

$$\hat{\theta} = \arg \min_{\theta = \{L_p, B, \sigma\}} \sum_i w_{m_{v,i}}(m_{v,i} - \hat{m}_{v,i})^2$$
$$+ \sum_j w_{c_{v,j}}(c_{v,j} - \hat{c}_{v,j})^2 \qquad (1)$$
$$+ \sum_k w_{c_{f,k}}(c_{f,k} - \hat{c}_{f,k})^2$$

$$J_w = L_p(\Delta P - \sigma \Delta \pi) \qquad (2)$$

$$J_s = B\Delta c, \begin{cases} B = constant & \text{for neutral membranes} \quad (3a) \\ B = \sum_{i \in I} b_i c_f{}^i & \text{for charged membranes} \quad (3b) \end{cases}$$

The Fisher information matrix (FIM), **M**, defined as the inverse of the parameter covariance matrix **V**, Eq. (4), is computed at the best fit parameter values $\hat{\theta}$ based on local sensitivities $\mathbf{Q}_r$ of the model predictions y_r to each parameter $\hat{\theta}$ at experimental conditions ϕ . The eigendecomposition of the FIM reveals which parameters are identifiable (Rothenberg, 1971).

$$\mathbf{M} = [\mathbf{V}(\hat{\theta}, \phi)]^{-1} = \sum_{r=1}^{N_y} \sum_{s=1}^{N_y} v_{m,rs}{}^{-1} \mathbf{Q}_r^T \mathbf{Q}_s,$$

$$\mathbf{Q}_r = \begin{bmatrix} \left.\frac{\partial y_r}{\partial \hat{\theta}_1}\right|_{t_1} & \cdots & \left.\frac{\partial y_r}{\partial \hat{\theta}_m}\right|_{t_1} \\ \vdots & \ddots & \vdots \\ \left.\frac{\partial y_r}{\partial \hat{\theta}_1}\right|_{t_n} & \cdots & \left.\frac{\partial y_r}{\partial \hat{\theta}_m}\right|_{t_n} \end{bmatrix} \qquad (4)$$

MBDoE techniques improve parameter precision by minimizing a metric of **V** or equivalently maximizing a metric of **M**. The most common criteria are the so-called

alphabetical design criteria, e.g., A-, D-, E-optimal criteria corresponding to minimizing the trace, the determinant, and the maximum eigenvalue of **V**, respectively (or maximizing the trace, the determinant, and the maximum eigenvalue of **M**). The determinant and trace of the covariance matrix **V** can be interpreted as the volume of the covariance ellipsoid under feasible experimental conditions, while the maximum eigenvalue represents the size of the major axis, minimizing them reduces the uncertainty of model parameters.

Results and Discussion

In this work, we apply the Fisher information matrix (FIM) analyses and MBDoE to further improve the DATA framework. We highlight two non-ideal phenomena, namely "lag" and "overflow", which occur when increasing the system pressure to the desired operating pressure, e.g., at the start of an experiment. Ideally, during the startup, the change in the pressure of the system is a step function and the increase in pressure brings the diafiltrate to the entrance of the stirred cell. However, in many cases, this is not physically realizable. If the targeted operating pressure is undershot, the diafiltrate does not make it to the entrance of the stirred cell on time - there is an extended amount of time ("lag" time) before the diafiltrate drips into the stirred cell. These conditions emulate a filtration experiment (without diafiltrate introduction), and lead to little change in concentration within the stirred cell c_f during the "lag" time. Dripping of diafiltrate into the stirred cell at the end of the "lag" time will cause a significant change in c_f. When the target operating pressure is overshot, bolus of diafiltrate enters the stirred cell, and causes a sudden increase in the retentate concentration c_f. This bolus is called the "overflow". Both phenomena lead to a change in the mass of solution in the stirred cell, m_f.

We extend the differential equation model proposed in DATA to consider both "lag" and "overflow" startup modes. For example, during "lag" time, no diafiltrate m_d enters the stirred cell while the solution in the stirred cell is still permeating, Eq. (5).

$$\frac{dm_f}{dt} = -\frac{dm_d}{dt} - A_m \rho J_w = -A_m \rho J_w \qquad (5)$$

where A_m is the membrane area, ρ is the density of the solution. Then the diafiltrate entering the stirred cell and the permeate leaving the stirred cell becomes steady with a slow air leaking, where the air volume in the stirred cell is slowly decreasing and the solution volume increases. We assume m_f is changing with a constant rate S over the experiment, Eq. (6). Initial and final m_f are measured to estimate S.

$$\frac{dm_f}{dt} = -\frac{dm_d}{dt} - A_m \rho J_w = S > 0 \qquad (6)$$

From FIM-based analyses, we find that modeling these phenomena can leverage the additional data (measurements of retentate concentration c_f) within the startup process to elucidate the physical system, i.e., the mass changing in the

stirred cell from Figure 2. The membrane performance characteristic parameters are identified with 5, 6, and 2 orders of magnitude increases in information content evaluated by A-, D-, E-optimality, respectively, and over one order of magnitude improvement in the precision of the parameters associated with solute permeability B. Perception of "lag" and "overflow" phenomena brings insights to design a time-varying applied pressure in DATA. A time correction for permeate product collected is also introduced to describe a time delay in the collecting tube, which improve the normalized residual squares of the three kinds of model predictions by 10% with "lag" or "overflow" start-up and 20% in the original DATA mode (which does not model startup).
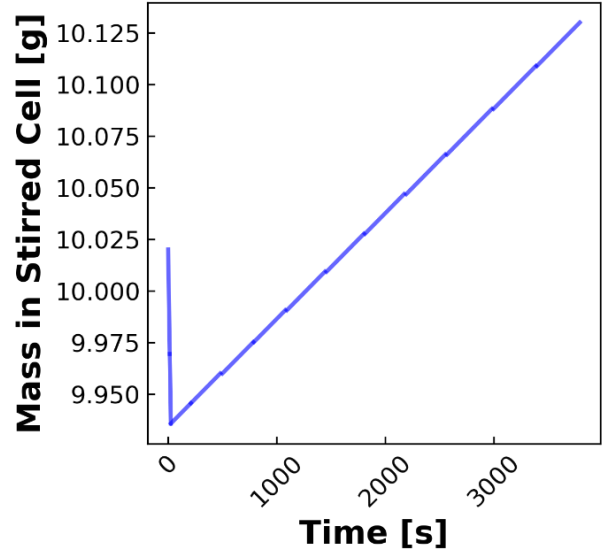

Figure 2. Mass changing in the stirred cell in "lag" mode

Next, we extend the DATA framework to investigate concentration-dependent membrane performance. We start by postulating a series of power law models, shown in Eq. (3b), to model how the solute permeability B depends on the feed side concentration c_f for surface-charged membranes. Different order polynomials $I \in [\{0, -0.5\}, \{0, 0.5\}, \{0, 1\}, \{0, 1, 2\}]$ were considered for Eq. (3b). Each set of I corresponds to different phenomenological models. For example, $I = \{0, 1\}$ can be related to models with Donnan equilibrium for charged membranes. Models with different I are compared to the original model, which assumes a constant solute permeability assumption, shown in Eq. (3a), that adequately describes the behavior of neutral membranes (Ouimet et al., 2022). Figures 3a and 3b show the best fit for the original model and proposed model ($I = \{0, 1, 2\}$). The proposed model improves permeate concentration predictions by 64% while preserving the quality of mass and retentate concentration predictions. Results for only the best fit model are reported here for brevity.
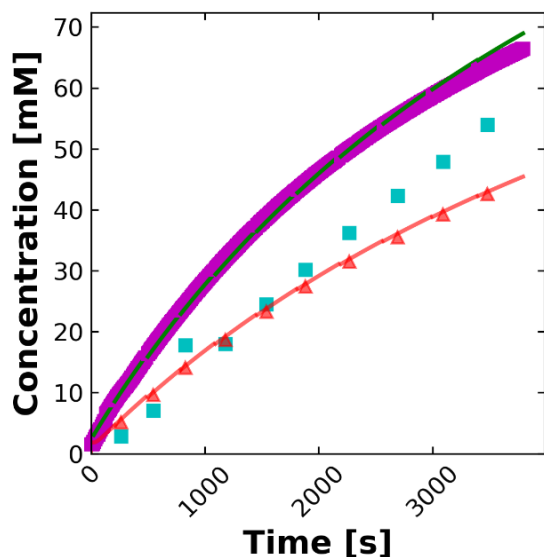
Figure 3a. Model inadequacy with constant solute permeability for charged membranes, Eq. (3a). $L_p = 9.75 \, L \cdot m^{-2} \cdot h^{-1} \cdot bar^{-1}$; $B = 9.50 \, \mu m \cdot s^{-1}$; $\sigma = 0.69$.
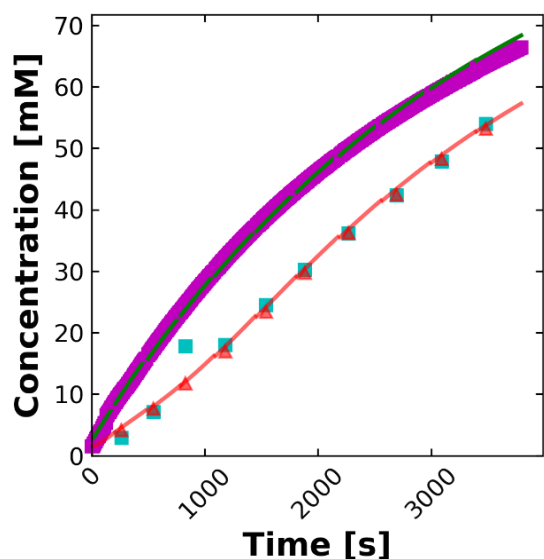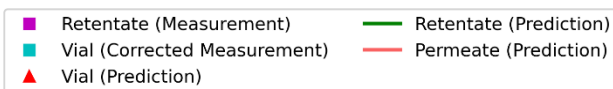

Figure 3b. Best fit model with concentration-dependent solute permeability for charged membranes, Eq. (3b). $L_p = 9.50 \, L \cdot m^{-2} \cdot h^{-1} \cdot bar^{-1}$; $B = 7.98 + 0.27c_f + 0.0087c_f{}^2 \, \mu m \cdot s^{-1}$ (c_f in unit of mM); $\sigma = 0.55$.

Conclusions and Future Opportunities

Charged membrane can offer selective transport of electrolytes, however, it is difficult to delve into a detailed understanding of the underlying phenomena, e.g., the molecular interactions between the charged functionality and the free ions in solution that affect the macroscopic transport properties. With the improved DATA, we are able to characterize the dependencies of membrane transport properties with high fidelity. The calibrated model is ready to be embedded in the scale-up, design, and optimization of separation systems with high computing performance.

The improved DATA also provides promising tools, including both hardware and data analytics workflows, to study the nanostructure-property-performance relationship for material design purposes by model discrimination between possible phenomena and mechanisms in the system. The best fit correlation model shown in Eq. (2b) acts as a good approximation of realities that can be applied to inform and select the phenomena combinations imported into model discrimination problems. As future work, we plan to develop a fully physics-based model that is analogous to the best fit instance ($I = \{0, 1, 2\}$) of Eq. (2b). Modeling the "lag" and "overflow" phenomena enables accurate prediction for future experiments with time-varying operating pressure, which could introduce more freedom in the design of experiments for both model discrimination and parameter precision problems.

Acknowledgments

References

Franceschini, G., & Macchietto, S. (2008). Model-based design of experiments for parameter precision: State of the art. *Chemical Engineering Science, 63*(19), 4846-4872.

Geise, G. M., Paul, D. R., & Freeman, B. D. (2014). Fundamental water and salt transport properties of polymeric

Ghosh, R., & Cui, Z. (2000). Analysis of protein transport and polarization through membranes using pulsed sample injection technique. *Journal of Membrane Science, 175*(1), 75-84.

Hoffman, J. R., & Phillip, W. A. (2020). 100th anniversary of macromolecular science viewpoint: integrated membrane systems. *ACS Macro Letters, 9*(9), 1267-1279.

Liu, X., Wang, J., Ouimet, J. A., Phillip, W., Dowling, A. (2022) Membrane characterization with model-based design of experiments. In *14th International Symposium on Process Systems Engineering*.

Muetzel, Z. W., Ouimet, J. A., & Phillip, W. A. (2022). Device for the Acquisition of Dynamic Data Enables the Rapid

Characterization of Polymer Membranes. *ACS Applied Polymer Materials, 4*(5), 3438-3447.

Ouimet, J. A., Liu, X., Brown, D. J., Eugene, E. A., Popps, T., Muetzel, Z. W., ... & Phillip, W. A. (2022). DATA: Diafiltration Apparatus for high-Throughput Analysis. *Journal of Membrane Science, 641,* 119743.

Rothenberg, T. J. (1971). Identification in parametric models. *Econometrica: Journal of the Econometric Society,* 577-591.

Sadeghi, I., Kaner, P., & Asatekin, A. (2018). Controlling and expanding the selectivity of filtration membranes. *Chemistry of Materials, 30*(21), 7328-7354.

Wang, J., & Dowling, A. W. (2022). Pyomo. DOE: An open-source package for model-based design of experiments in Python. *AIChE Journal*, e17813.

Yaroshchuk, A., Bruening, M. L., & Zholkovskiy, E. (2019). Modelling nanofiltration of electrolyte solutions. *Advances in Colloid and Interface Science, 268*, 39-63.